

pubs.acs.org/est Article

Influence of Mechanical Ventilation Systems and Human Occupancy on Time-Resolved Source Rates of Volatile Skin Oil Ozonolysis Products in a LEED-Certified Office Building

Tianren Wu, Antonios Tasoglou, Heinz Huber, Philip S. Stevens, and Brandon E. Boor*



Cite This: Environ. Sci. Technol. 2021, 55, 16477-16488



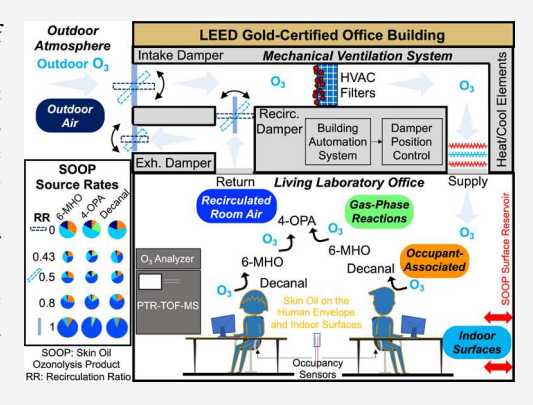
ACCESS

Metrics & More

Article Recommendations

Supporting Information

ABSTRACT: Building mechanical ventilation systems are a major driver of indoor air chemistry as their design and operation influences indoor ozone (O_3) concentrations, the dilution and transport of indoor-generated volatile organic compounds (VOCs), and indoor environmental conditions. Real-time VOC and O_3 measurements were integrated with a building sensing platform to evaluate the influence of mechanical ventilation modes and human occupancy on the dynamics of skin oil ozonolysis products (SOOPs) in an office in a LEED-certified building during the winter. The ventilation system operated under variable recirculation ratios (RRs) from RR = 0 (100% outdoor air) to RR = 1 (100% recirculation air). Time-resolved source rates for 6-methyl-5-hepten-2-one (6-MHO), 4-oxopentanal (4-OPA), and decanal were highly dynamic and changed throughout the day with RR and occupancy. Total SOOP source rates during high-occupancy periods (10:00–18:00) varied from 2500–3000 μ g h⁻¹ when RR = 0.1 to 6300–6700 μ g h⁻¹ when RR = 1. Source rates for gas-phase



reactions, outdoor air, and occupant-associated emissions generally decreased with increasing RR. The recirculation air source rate increased with RR and typically became the dominant source for RR > 0.5. SOOP emissions from surface reservoirs were also a prominent source, contributing 10-50% to total source rates. Elevated per person SOOP emission factors were observed, potentially due to multiple layers of soiled clothing worn during winter.

KEYWORDS: indoor air quality, volatile organic compounds, proton transfer reaction time-of-flight mass spectrometry, high-performance buildings, ozone chemistry

INTRODUCTION

Ozone (O₃) is a prominent gas-phase oxidant in the indoor environment and is associated with numerous adverse health outcomes. It can readily react with compounds in human skin oil that contain unsaturated carbon bonds, such as squalene, glycerides, fatty acids, and cholesterols, resulting in the formation of volatile skin oil ozonolysis products (SOOPs).^{2,3} Volatile SOOPs include a series of carbonyl compounds that can affect indoor air quality and participate in gas-phase chemistry. Some SOOPs exhibit high product yields, such as acetone, geranyl acetone (GA), 6-methyl-5-hepten-2one (6-MHO), 4-oxopentanal (4-OPA), methacrolein/methyl vinyl ketone, and decanal.^{2,4} SOOP product yields are highly variable among individuals.⁴ Ozonolysis of human skin oil represents an important class of indoor chemical reactions that can act as a near-continuous source of volatile organic compounds (VOCs) in occupied environments. Some of the produced SOOPs are odorous^{1,5} (e.g., decanal), have been identified as occupational asthma hazards⁶ (e.g., 4-OPA), can cause irritation of the respiratory system and skin⁷⁻⁹ (e.g., 4-OPA), and can enhance the mass of indoor aerosols 10 (e.g., 6MHO). The reactions can produce condensed products on skin surfaces³ that may penetrate through the skin. ^{11–15}

Indoor O₃ and SOOP chemistry in mechanically ventilated buildings can be strongly influenced by the design and operation of heating, ventilation, and air conditioning (HVAC) systems. HVAC systems serve as an important interface between indoor and outdoor atmospheres. HVAC units in modern commercial buildings include advanced building automation systems with complex control logic that can modulate their operational modes based on thermal conditions, energy use, and occupancy, among other factors. The mechanical ventilation mode can change dynamically across variable time scales, from minutes to hours to seasons, according to the conditions of indoor and outdoor

Received: May 13, 2021 Revised: August 31, 2021 Accepted: October 21, 2021 Published: December 1, 2021





air, such as temperature, relative humidity (RH), and carbon dioxide (CO_2) concentrations. HVAC systems are expected to strongly impact SOOP source and loss processes as the ventilation mode governs the delivery rate of outdoor O_3 and the dilution and transport of indoor-generated VOCs.

The application of proton transfer reaction time-of-flight mass spectrometry (PTR-TOF-MS) has facilitated the characterization of the fate and transport of SOOPs in occupied indoor environments. Time-resolved SOOP measurements have been conducted in simulated chambers, 2,19-22 a university classroom, ^{23,24} an art museum, ²⁵ a movie theater, ²⁶ an athletic center,²⁷ and a residential house.^{28,29} These studies have provided new fundamental insights into factors that affect indoor SOOP concentrations. However, real-time PTR-TOF-MS measurements of indoor SOOPs in office buildings and under variable mechanical ventilation conditions are limited. Time-dependent changes in both the operation of mechanical ventilation systems and human occupancy patterns may change the rate of production of volatile SOOPs in modern offices. Evaluation of how HVAC control strategies and operational factors affect SOOP dynamics in office buildings can guide engineering control strategies for reducing indoor exposure to SOOPs in these environments.

The objectives of this study are to integrate multilocation PTR-TOF-MS measurements with a kinetic material balance model to estimate source rates ($\mu g h^{-1}$) of three major SOOPs (6-MHO, 4-OPA, and decanal) in an occupied open-plan office and to investigate how source-specific source rates change with mechanical ventilation conditions and office occupancy. Volatile SOOPs were measured in real-time (1 Hz) with a PTR-TOF-MS in one of the four Living Laboratory (LL) offices at the Purdue University Ray W. Herrick Laboratories. The LL offices are part of a high-performance building that was awarded a LEED Gold Certificate. The building was designed and constructed following criteria for future high-performance buildings and includes a state-of-theart building automation and sensing platform, energy-efficient HVAC technologies, and low-VOC-emitting building materials and furnishings. The extensive monitoring and control of the HVAC system and office space provides a basis for new insights into the influence of dynamic mechanical ventilation modes and occupancy patterns on indoor O₃ and SOOP chemistry in a modern office building.

MATERIALS AND METHODS

Site Description: Herrick Living Laboratory Offices at Purdue University. The measurement campaign was conducted from February 14 to March 18, 2019 in one of the four Herrick LL offices in West Lafayette, IN, USA. The volume of each LL office is 333 m³, and the maximum occupancy is 20. The HVAC system is precisely controlled through an advanced building automation system, and the ventilation parameters are characterized in real-time by an extensive array of sensors. The LL office supply air contains a mixture of outdoor air and recirculated room air (Figure S1). The ratio of the recirculation volumetric airflow rate to the supply volumetric airflow rate, referred to as the recirculation ratio (RR), was determined by the control logic and varied between 0 (100% outdoor air) and 1 (100% recirculated room air).

The HVAC system operated under its pre-existing mode for 25 days, which represents the normal control logic for the LL offices, and in override mode for 9 days, where we deliberately

maintained the RR at 0 or 1. Under the pre-existing mode, the dampers automatically modulate to adjust the outdoor and recirculation volumetric airflow rates to maintain the mixed recirculation and outdoor air at predetermined set points according to the outdoor and room air temperatures while maintaining a minimum outdoor airflow of 0.12 m³ s⁻¹. The outdoor air temperature varied between -7 and 11.5 °C (5-95 percentiles), and the HVAC system operated under heating mode during the campaign. The fixed mixed air temperature set points make the supply air temperature more controllable after passing through the heating and cooling coils. The set point of mixed air was 8.8 °C from February 14 to February 25, 17.2 °C from February 26 to March 6, and 17.2 °C from March 15 to March 18 (Figure S2), which were determined by the design engineers of the building automation system. The RR was deliberately maintained at 1 from March 6 to March 13 and at 0 from March 13 to March 15 to explore the dynamics of SOOPs under each mechanical ventilation condition.

During the campaign, the mean volumetric airflow rates of the supply and return air were 0.65 (\pm 0.05) and 0.66 (\pm 0.05) m³ s⁻¹, respectively, equivalent to a mean air exchange rate (AER) of 7.1 h⁻¹. There is a room air CO₂ concentration threshold of 900 ppm, above which the system will gradually increase the outdoor volumetric airflow rate. However, this threshold was never exceeded under the pre-existing mode. The mean RH was 21.2 (\pm 8.1)%. Additional details about the LL offices and their HVAC systems can be found in the Supporting Information (SI).

Measurements and Instrumentation. VOC concentrations were measured by a proton transfer reaction time-offlight mass spectrometer (PTR-TOF-MS; PTR-TOF 4000, Ionicon Analytik Ges.m.b.H., Innsbruck, Austria) with hydronium (H₃O⁺) serving as the primary reagent ion. The PTR-TOF-MS was connected to a continuously purged automated valve system, which enabled sampling of supply, return, and outdoor air, along with several other sampling locations throughout the HVAC system (Figure S1). The return air was sampled in the duct 1.2 m downstream of the return air grille in the LL office, which represents the room air. O₃ and CO₂ concentrations were monitored by an O₃ gas analyzer (M400E, Teledyne Technologies Inc., Thousand Oaks, CA, USA) and a CO₂ gas analyzer (LI-830, LI-COR Biosciences, Lincoln, NE, USA), respectively. Human occupancy was monitored through a chair-based temperature sensor array with a time resolution of 15 s;³⁰ this enabled investigation of dynamic VOC emissions from the human envelope. Details of the settings of the automated valve system, calibration of the PTR-TOF-MS, and concentration calculations for 6-MHO, 4-OPA, and decanal can be found in the SI.

Material Balance Model for Characterizing SOOP Source and Loss Processes. A material balance model was developed to quantify time-resolved source rates of 6-MHO, 4-OPA, and decanal in the LL office. The room air is assumed to be well mixed. The following differential equation (eq 1) describes time-dependent changes in the concentration of a compound in the room due to mechanical ventilation, infiltration through the building envelope, indoor surface partitioning, emissions from the human envelope via ozonolysis of skin oil, and gas-phase reactions

$$\frac{V \text{ d}[C]}{\text{d}t} = Q_{\text{supply}}(t) \times [C]_{\text{supply}} - Q_{\text{return}}(t) \times [C]$$

$$+ Q_{\text{infiltration}} \times [C]_{\text{outdoor}} - Q_{\text{exfiltration}} \times [C]$$

$$+ n(t) \times E_{\text{occupant}}(t) + R(t) + P_{\text{surface}}(t)$$
 (1)

where V is the room volume (m^3) , [C] is the well-mixed room air concentration of the compound of interest $(mol\ m^{-3})$; measured in the return air), $[C]_{\text{supply}}$ is the concentration in the supply air $(mol\ m^{-3})$, $[C]_{\text{outdoor}}$ is the concentration in the outdoor air $(mol\ m^{-3})$, $Q_{\text{supply}}(t)$ is the supply volumetric airflow rate $(m^3\ s^{-1})$, $Q_{\text{infiltration}}$ is the infiltration volumetric airflow rate $(m^3\ s^{-1})$, $Q_{\text{exfiltration}}$ is the exfiltration volumetric airflow rate $(m^3\ s^{-1})$, n(t) is the number of office workers, $E_{\text{occupant}}(t)$ is the per person emission rate of the compound from the human surface envelope via ozonolysis reactions $(mol\ s^{-1})$, R(t) is the production rate minus the loss rate via gas-phase chemical reactions $(mol\ s^{-1})$, and $P_{\text{surface}}(t)$ is the emission rate from indoor surfaces minus the surface deposition rate $(mol\ s^{-1})$.

 $Q_{\text{supply}}(t)$ and $Q_{\text{return}}(t)$ were retrieved from the building automation system with a time resolution of 1 min. $Q_{\text{infiltration}}$ and $Q_{\text{exfiltration}}$ were determined via CO_2 concentration decay during unoccupied periods with mean values of 0.336 and 0.286 h⁻¹, respectively. $Q_{\text{infiltration}}$ was not equal to $Q_{\text{exfiltration}}$ as the HVAC system maintained the office at a slight negative pressure.

 $n(t) \times E_{\rm occupant}(t)$ represents the total emission rate in the room via ozonolysis reactions at the human surface envelope when the occupancy is n(t), which changes with time. It assumes that the amount of skin oil and other condensed-phase precursors available for reactions is proportional to occupancy. We treat the term dynamically in order to capture minute-to-minute variations in occupancy. We assume that $E_{\rm occupant}(t)$ varies with the O_3 concentration in the room; therefore, it is expressed as 31

$$E_{\text{occupant}}(t) = k_{\text{app},i}[O_3] \tag{2}$$

where $[O_3]$ is the O_3 concentration (mol m⁻³) and $k_{\text{app},i}$ is the apparent reaction rate constant for product i (m³ s⁻¹). We considered the emission of all three SOOPs via ozonolysis reactions at the human surface envelope.

The following gas-phase chemical reactions were considered: the formation of 6-MHO and 4-OPA from the reaction between O_3 and GA and the loss of 6-MHO and formation of 4-OPA from the reaction between O_3 and 6-MHO. Therefore, gas-phase chemical reaction terms for 6-MHO and 4-OPA are expressed as eqs 3 and 4, 15 while we assume there is no gas-phase reaction that took place for decanal

$$R_{6\text{MHO}}(t) = \frac{1}{2}Vk_1[O_3][GA] - Vk_2[O_3][6\text{MHO}]$$
(3)

$$R_{4\text{OPA}}(t) = \frac{1}{2} V k_1 [O_3] [GA] + V k_2 [O_3] [6MHO]$$
(4)

The reaction rate constants k_1 and k_2 were retrieved from the EPI suite³² assuming a temperature of 25 °C. k_1 is 8.6×10^{-16} cm³ s⁻¹ (5.18 × 10² m³ mol⁻¹ s⁻¹), and k_2 is 4.3×10^{-16} cm³ s⁻¹ (2.59 × 10² m³ mol⁻¹ s⁻¹).

The term $P_{\text{surface}}(t)$ describes the emission^{23,25} from and deposition^{25,31} to indoor surfaces. In this study, we found that the decay of 6-MHO, 4-OPA, and decanal starting from the

beginning of the unoccupied periods did not exhibit a rate greater than the ventilation rate and followed the ventilation rate well (Figure S3). Thus, we treated $P_{\rm surface}(t)$ as a constant net surface emission rate, $E_{\rm surface}$.

On the basis of these assumptions, the governing equations for 6-MHO, 4-OPA, and decanal can be expressed as

$$\begin{split} \frac{V \text{ d[6MHO]}}{\text{d}t} &= Q_{\text{supply}}(t) \times [6\text{MHO}]_{\text{supply}} \\ &- Q_{\text{return}}(t) \times [6\text{MHO}] \\ &+ Q_{\text{infiltration}} \times [6\text{MHO}]_{\text{outdoor}} \\ &- Q_{\text{exfiltration}} \times [6\text{MHO}] \\ &+ n(t) \times k_{\text{app,6MHO}}[O_3] + \frac{1}{2}Vk_1[O_3][\text{GA}] \\ &- Vk_2[O_3][6\text{MHO}] + E_{\text{surface,6MHO}} \end{split}$$
 (5)

$$\frac{V \text{ d[4OPA]}}{\text{d}t} = Q_{\text{supply}}(t) \times [4\text{OPA}]_{\text{supply}}$$

$$- Q_{\text{return}}(t) \times [4\text{OPA}] + Q_{\text{infiltration}}$$

$$\times [4\text{OPA}]_{\text{outdoor}} - Q_{\text{exfiltration}} \times [4\text{OPA}]$$

$$+ n(t) \times k_{\text{app,4OPA}}[O_3] + \frac{1}{2}Vk_1[O_3][GA]$$

$$+ Vk_2[O_3][6\text{MHO}] + E_{\text{surface,4OPA}}$$
 (6)

$$\begin{split} \frac{V \text{ d[Decanal]}}{\text{d}t} &= Q_{\text{supply}}(t) \times [\text{Decanal}]_{\text{supply}} \\ &- Q_{\text{return}}(t) \times [\text{Decanal}] \\ &+ Q_{\text{infiltration}} \times [\text{Decanal}]_{\text{outdoor}} \\ &- Q_{\text{exfiltration}} \times [\text{Decanal}] \\ &+ n(t) \times k_{\text{app,Decanal}}[O_3] + E_{\text{surface,Decanal}} \end{split}$$

The unknown parameters in eqs 5-7 are $E_{\text{surface,6MHO}}$, $E_{
m surface, 4OPA}$, $E_{
m surface, Decanal}$, $k_{
m app, 6MHO}$, $k_{
m app, 4OPA}$, and $k_{
m app, Decanal}$, while the remaining parameters were directly measured. The net surface emission rates ($E_{\text{surface,6MHO}}$, $E_{\text{surface,4OPA}}$, and $E_{\text{surface},Decanal}$) were obtained each day during the unoccupied periods (n = 0) before the start of the occupied periods²³ using a nonlinear least-squares curve-fitting function (lsqcurvefit.m) in MATLAB (The MathWorks Inc., Natick, MA, USA). This was done to avoid direct emissions from the human envelope. We assume these values are constant on the day of interest and applied them to the occupied periods. Then, the SOOP apparent reaction rate constants ($k_{\rm app,6MHO}$, $k_{\rm app,4OPA}$, and $k_{\text{app,Decanal}}$) were determined via nonlinear least-squares curve fitting with a time step of 1 min. The fitting quality is shown in Figures S6-S8. The gas-phase reactions of the SOOPs with hydroxyl and nitrate radicals were not considered due to their low concentrations in typical indoor environments. 25,33-36

SOOP Source Rates Apportioned by Source Type. SOOP source rates (μ g h⁻¹) for: (1) outdoor air ($S_{\text{outdoor},i}$), (2) recirculation air ($S_{\text{recirc},i}$), (3) human surface envelope emissions ($S_{\text{human},i}$), (4) indoor surface emissions ($S_{\text{surface},i}$), and (5) gas-phase reactions ($S_{\text{gas-rxn},i}$) under different ventilation and occupancy conditions were calculated. The source rates were estimated as the integral of the VOC flux

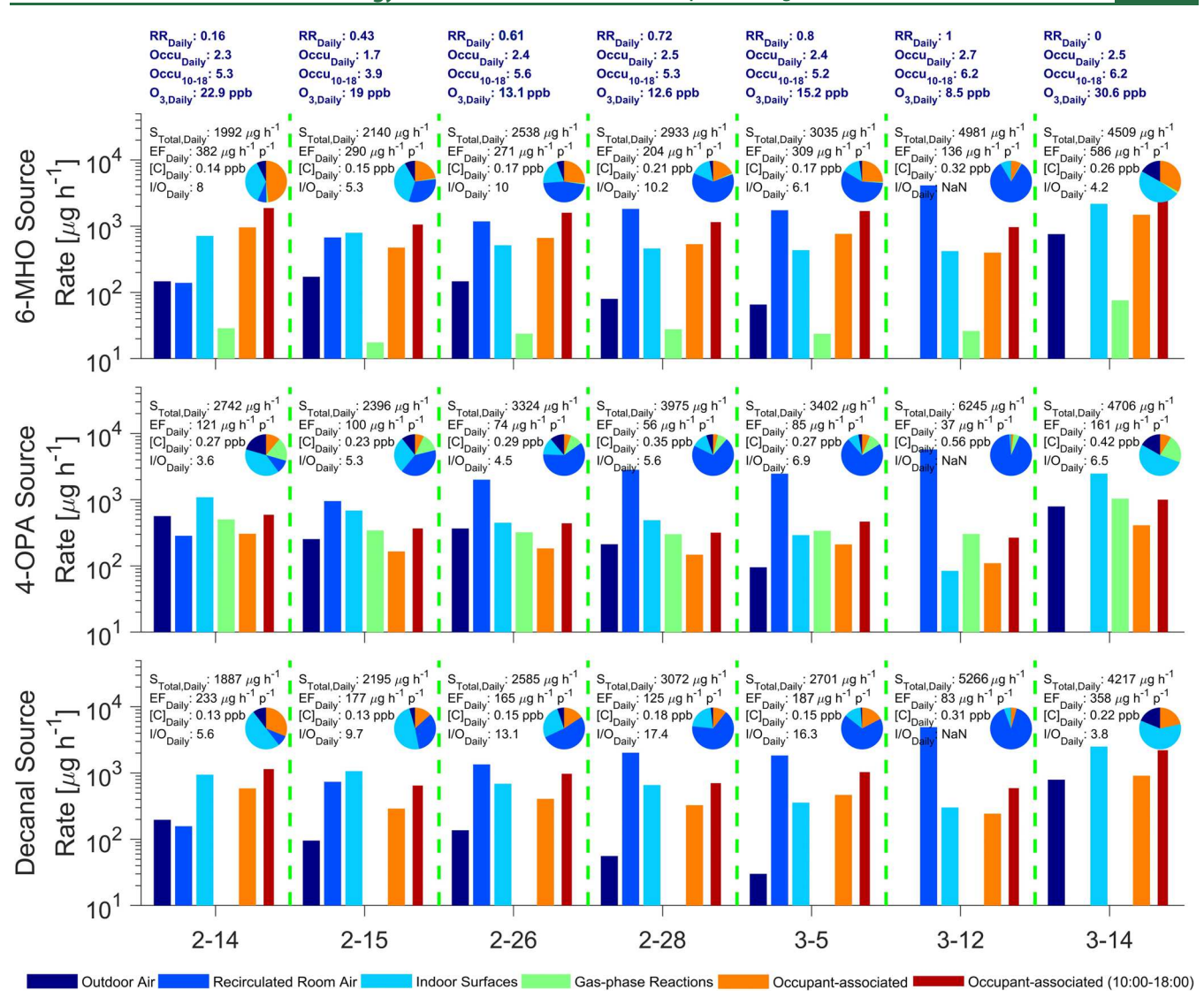


Figure 1. Daily mean (24-h average) source rates for 6-MHO, 4-OPA, and decanal and their apportionment by source type. Pie charts represent the relative contribution of each source type to the total SOOP source rate. RR_{Daily} is the daily mean recirculation ratio, $Occu_{Daily}$ is the daily mean office occupancy, $Occu_{10-18}$ is the mean office occupancy during high-occupancy periods (10:00–18:00), $O_{3,Daily}$ is the daily mean indoor O_3 concentration, $S_{Total,Daily}$ is the daily mean total SOOP source rate, EF_{Daily} is the daily mean per person SOOP emission factor, $[C]_{Daily}$ is the daily mean indoor SOOP concentration, and I/O_{Daily} is the daily mean SOOP indoor/outdoor ratio. Additional details can be found in Tables S2–S4.

from different sources over a given period. The daily source rates were estimated as

$$\begin{split} S_{\text{outdoor},i} &= \int_{t_0}^{t_1} Q_{\text{supply}}(t) \times [C]_{\text{supply}} \text{d}t \\ &\times \frac{Q_{\text{outdoor}}(t) \times [C]_{\text{outdoor}}}{Q_{\text{outdoor}}(t) \times [C]_{\text{outdoor}} + Q_{\text{recirc}}(t) \times [C]_{\text{recirc}}} \\ &\times \frac{1}{t_1 - t_0} \end{split} \tag{8}$$

$$\begin{split} S_{\text{recirc},i} &= \int_{t_0}^{t_1} Q_{\text{supply}}(t) \times [C]_{\text{supply}} \text{d}t \\ &\times \frac{Q_{\text{recirc}}(t) \times [C]_{\text{recirc}}}{Q_{\text{outdoor}}(t) \times [C]_{\text{outdoor}} + Q_{\text{recirc}}(t) \times [C]_{\text{recirc}}} \\ &\times \frac{1}{t_1 - t_0} \end{split}$$

$$S_{\text{human},i} = \int_{t_0}^{t_1} n(t) k_{\text{app},i} [O_3] dt \times \frac{1}{t_1 - t_0}$$
 (10)

$$S_{\text{surface},i} = E_{\text{surface},i} \tag{11}$$

$$S_{\text{gas-rxn},6\text{MHO}} = \int_{t_0}^{t_1} \frac{1}{2} V k_1 [O_3] [GA] dt \times \frac{1}{t_1 - t_0}$$
 (12)

$$S_{\text{gas-rxn,4OPA}} = \int_{t_0}^{t_1} \left(\frac{1}{2} V k_1 [O_3] [GA] + V k_2 [O_3] [6MHO] \right) dt$$

$$\times \frac{1}{t_1 - t_0}$$
(13)

where t_0 and t_1 represent the start and end times of the period of interest, respectively; $Q_{\rm recirc}(t)$ is the recirculation volumetric airflow rate (m³ s⁻¹), which equals $Q_{\rm return}(t) \times RR$; $Q_{\rm outdoor}(t)$ is the outdoor volumetric airflow rate (m³ s⁻¹); and $[C]_{\rm recirc}$ is the concentration in the recirculated air (mol m⁻³), which is assumed to be the same as the well-mixed room air

concentration. The summation of the source-specific source rates is the total source rate for each SOOP (S_{total}). Daily mean per person SOOP emission factors (EF, μ g h⁻¹ p⁻¹) were estimated as the ratio of the integral of S_{human} to the integral of the occupancy over the day of interest.

Ozone Deposition Velocity. When estimating the O_3 deposition velocity (cm s⁻¹) for indoor surfaces in the LL office, the gas-phase reactions of O_3 with 6-MHO, GA, and monoterpenes were also considered. The O_3 deposition velocity to indoor surfaces was calculated during unoccupied periods using the following equation

$$\frac{V \text{ d}[O_3]}{\text{d}t} = Q_{\text{supply}}(t) \times [O_3]_{\text{supply}} - Q_{\text{return}}(t) \times [O_3]$$

$$+ Q_{\text{infiltration}} \times [O_3]_{\text{outdoor}} - Q_{\text{exfiltration}} \times [O_3]$$

$$- A_{\text{room}} \times v_{\text{dep,room}}[O_3] - Vk_1[O_3][GA]$$

$$- Vk_2[O_3][6MHO]$$

$$- Vk_3[O_3][Monoterpenes]$$
(14)

where $A_{\rm room}$ is the surface area of the office (705 m²), $\nu_{\rm dep,room}$ is the O₃ deposition velocity to indoor surfaces (cm s⁻¹), k_3 is the reaction rate constant between O₃ and monoterpenes, and [Monoterpenes] is the monoterpene concentration as measured by the PTR-TOF-MS. The remaining parameters are defined in the main text. k_3 was adopted from a previous study. $\nu_{\rm dep,room}$ was obtained using a nonlinear least-squares curve-fitting function. Then, the per person O₃ deposition velocity (cm s⁻¹ p⁻¹) was estimated during the occupied periods using the following equation

$$\frac{V \text{ d}[O_3]}{\text{d}t} = Q_{\text{supply}}(t) \times [O_3]_{\text{supply}} - Q_{\text{return}}(t) \times [O_3]$$

$$+ Q_{\text{infiltration}} \times [O_3]_{\text{outdoor}} - Q_{\text{exfiltration}} \times [O_3]$$

$$- A_{\text{room}} \times \nu_{\text{dep,room}}[O_3] - n(t) \times A_{\text{human}}$$

$$\times \nu_{\text{dep,human}}[O_3] - Vk_1[O_3][GA]$$

$$- Vk_2[O_3][6MHO]$$

$$- Vk_3[O_3][Monoterpenes]$$
(15)

where $A_{\rm human}$ is the surface area of an occupant $(1.7 \text{ m}^2)^{31,37}$ and $\nu_{\rm dep,human}$ is the per person O_3 deposition velocity onto the surface envelope of the human body (cm s⁻¹ p⁻¹). $\nu_{\rm dep,human}$ was calculated using a nonlinear least-squares curve-fitting function after $\nu_{\rm dep,room}$ was obtained.

■ RESULTS AND DISCUSSION

The LL office recirculation ratio (RR) ranged from 0.1 to 0.84 under the pre-existing HVAC operational mode and was set to 0 and 1 under the override mode during the measurement campaign. Here, the results are presented from selected days under both modes to demonstrate the significant influence of building mechanical ventilation modes and human occupancy on temporal variations in SOOP source rates and the relative contribution of each SOOP source type.

Daily Mean SOOP Source Rates and Apportionment by Source Type for the Living Laboratory Office. Figure 1 presents the daily mean SOOP source rates and their apportionment on selected days with different RRs for the LL office HVAC system. The pie charts show the relative

contribution of each source to the total source rate (S_{total}). The source rates were estimated as daily averages due to the continuous operation of the HVAC system and the extended periods of occupancy, often spanning from 7 AM to 12 AM. The source-specific SOOP source rates presented here can be used in modeling studies to predict indoor SOOP concentrations under different mechanical ventilation and occupancy conditions. Additional details regarding the SOOP source rates and LL office conditions for each day can be found in Tables S2–S4.

The outdoor SOOP concentrations exhibited relatively small temporal variations compared to indoor concentrations. Therefore, the value of the outdoor source term (S_{outdoor}) mainly scales with the outdoor volumetric airflow rate $(Q_{\text{outdoor}}(t))$. S_{outdoor} shows maximum values of 761–794 μ g h^{-1} for the three SOOPs on March 14 when RR = 0 (100%) outdoor air), with a relative contribution of up to 0.19 to S_{total} . The recirculation source rate (S_{recirc}) increased significantly from 139-285 μ g h⁻¹ on February 14 when RR = 0.16 to $4131-5743 \mu \text{g h}^{-1}$ on March 12 when RR = 1 (100%) recirculated room air). The magnitude of S_{recirc} is affected by the recirculation airflow rate and indoor SOOP concentrations, the latter of which is also influenced by other sources. The rise in RR not only increases the recirculation airflow rate, but decreases the amount of outdoor air available for dilution, thereby leading to higher indoor SOOP concentrations. The daily mean relative contribution of S_{recirc} to S_{total} gradually increased with RR (Table S4). S_{recirc} typically became the dominant source for SOOPs for RR > 0.5 and contributed 0.86-0.94 to S_{total} when RR = 1.

The source rate of human surface envelope emissions (S_{human}) is primarily influenced by office occupancy and indoor O₃ concentrations. The daily mean occupancy varied within a narrow range during the selected days shown in Figure 1 (2.3-2.7), aside from February 15 when it was 1.7. As the RR decreases, the outdoor O₃ delivery rate generally increases, thereby resulting in higher indoor O₃ concentrations (Figure S5) that led to an increase in S_{human} . The highest daily mean values were found on March 14 when RR = 0 (100% outdoor air), with $S_{\text{human}} = 1493$, 410, and 912 μ g h⁻¹ for 6-MHO, 4-OPA, and decanal, respectively. The lowest values were observed on March 12 when RR = 1 (100% recirculated room air). On this day, the lowest daily mean indoor concentration of O_3 was observed (8.5 ppb, Table S2). Under RR = 1, outdoor O_3 entered the LL office via infiltration through the building envelope $(Q_{infiltration} = 0.336 \text{ h}^{-1}).^{38}$ The daily mean relative contribution of human surface envelope emissions to the total source rate varied between 0.08 and 0.46 for 6-MHO and 0.05 and 0.27 for decanal, while it was only between 0.02 and 0.11 for 4-OPA (Table S4). The latter indicates that emissions of 4-OPA from the human envelopes of the office occupants are relatively small, possibly due to the low fraction of 4-OPA precursors that are surface bound due to their high volatility.2,14,15

The source rate of the gas-phase reactions ($S_{\rm gas-rxn}$) is influenced by indoor concentrations of O₃ and gas-phase precursors, which are partially influenced by the RR and LL office occupancy. The daily mean $S_{\rm gas-rxn}$ of 6-MHO varied between 18 and 76 μ g h⁻¹ and contributed only up to 0.02 to $S_{\rm total}$ (Tables S2 and S4). $S_{\rm gas-rxn}$ for 4-OPA showed a relative contribution of 0.05–0.22 to $S_{\rm total}$, with $S_{\rm gas-rxn}$ reaching a maximum value of 1035 μ g h⁻¹ when RR = 0 and a minimum

value of 221 μ g h⁻¹ when RR = 0.82. $S_{gas-rxn}$ was not considered for decanal.

The highest daily mean $S_{\rm total}$ was observed when RR = 1 on March 12, with $S_{\rm total}$ ranging from 4981 to 6245 μ g h⁻¹ among the three SOOPs. Interestingly, the second highest $S_{\rm total}$ was found when RR = 0 on March 14, since the enhanced $S_{\rm outdoor}$, $S_{\rm human}$, and $S_{\rm gas-rxn}$ driven by the high outdoor volumetric airflow rate and O_3 concentration coincided with significant emissions from indoor surfaces (see subsequent discussion). The lowest $S_{\rm total}$ for 6-MHO, 4-OPA, and decanal were 1992, 2396, and 1887 μ g h⁻¹, respectively, observed when RR = 0.16 for 6-MHO and decanal and when RR = 0.43 for 4-OPA.

 S_{total} during high-occupancy periods (10:00–18:00) was 10–80% greater than the daily means due to the increased abundance of precursors (Table S3). These factors increase S_{recirc} , S_{human} , and $S_{\text{gas-rxn}}$. S_{total} during the high-occupancy periods reached 6259–6743 μ g h⁻¹ for the three SOOPs, observed when RR = 1. S_{human} generally doubled or even tripled during high-occupancy periods with a relative contribution to S_{total} of 0.16–0.62, 0.04–0.19, and 0.1–0.41 for 6-MHO, 4-OPA, and decanal, respectively (Table S4).

Tang et al. (2016)²³ reported source rates for 6-MHO and 4-OPA in a university classroom with a single-pass ventilation system that operated with 100% outdoor air (RR = 0). The median supply air source rates for 6-MHO and 4-OPA as reported by Tang et al. (2016) were approximately 25% and 70% higher than the values of S_{outdoor} in this study when RR = 0. This is partially due to the higher outdoor volumetric airflow rate for the classroom. The median indoor nonoccupant source rate in the classroom was similar to the sum of the gas-phase reaction source rate and surface emission source rate during the high-occupancy period on February 14 when RR = 0.16. The occupant-related source rate for 6-MHO in the classroom agrees well with S_{human} during the high-occupancy period on March 14 when RR = 0, and that for 4-OPA is 2-fold greater. However, the mean occupancy in the classroom was 49, while the mean occupancy in the LL office during the highoccupancy period on March 14 was 6.2. The daily mean S_{total} values in this study were generally lower than the median total source rates reported by Tang et al. (2016), aside from March 12 when RR = 1 and March 14 when RR = 0.

Per-Person SOOP Emission Factors for Office Occupants. Daily mean per person SOOP emission factors (EFs) generally increased with the daily mean indoor O3 concentration as occupant-associated SOOP emission rates were estimated as a function of the indoor O₃ concentration (eq 2). The lowest daily mean SOOP EFs were observed on March 12 when RR = 1 and O_3 = 8.5 ppb, with EF = 136, 37, and 83 μ g h⁻¹ p⁻¹ for 6-MHO, 4-OPA, and decanal, respectively. The highest daily mean SOOP EFs were observed on March 14 when RR = 0 and O_3 = 30.6 ppb, with EF= 586, 161, and 358 μ g h⁻¹ p⁻¹ for 6-MHO, 4-OPA, and decanal, respectively. The mean EFs aggregated across all days and RRs were 301, 86, and 183 μ g h⁻¹ p⁻¹ for 6-MHO, 4-OPA, and decanal, respectively. The EFs for 6-MHO and 4-OPA estimated in this study are significantly higher than those reported for a university classroom in California in November (6-MHO, 99.3 µg h⁻¹ p^{-1} ; 4-OPA, 36.9 μ g h^{-1} p^{-1})²³ and a university art museum in Colorado in May (6-MHO, 18 μ g h⁻¹ p⁻¹; 4-OPA 22 μ g h⁻¹ p⁻¹). Conversely, Finewax et al. (2020)²⁷ reported high EFs for 6-MHO in the weight room of a university athletic center, which spanned from approximately 100 to 500 μ g h⁻¹ p⁻¹ with a median of 134 μ g h⁻¹ p⁻¹. The authors attributed the

elevated 6-MHO EFs to greater exposed skin area, soiled clothing, and reduced thickness of the body surface boundary layer during exercise, which facilitates O₃ consumption and increased sebum production.

The O₃ deposition velocity to indoor surfaces in the LL office during unoccupied periods was 0.045 cm s⁻¹ (Table S1), consistent with prior indoor observations. 1,39 However, the mean per person O₃ deposition velocity was 1.35 cm s⁻¹ p⁻¹ (calculated by assuming a surface area of the human surface envelope of 1.7 m²),^{31,37} which is 3–6-fold greater than values reported in an art museum,²⁵ university classroom,³¹ simulated office, 2,40 and simulated aircraft cabin 41 and about 50% higher than that reported in the athletic center.²⁷ We estimated the SOOP molar yields as the ratio of the molar EF to the per person O₃ molar consumption (excluding the consumption by indoor surfaces) (Table S1). The mean molar yield for 6-MHO is 0.048 (\pm 0.021), similar to that reported by Salvador et al. (2019) $(0.013-0.044)^{20}$ Yang et al. (2016) $(0.02 \pm 1)^{20}$ $(0.003)^{42}$ and Finewax et al. $(2020)(0.027 \pm 0.007)^{27}$ while much smaller than that reported by Morrison et al. (2021)⁴ (0.184-0.279) and Wisthaler and Weschler (2010) (0.16).² The mean molar yields for 4-OPA and decanal were 0.018 (± 0.0071) and 0.024 (± 0.01) , respectively, similar to those reported by Morrison et al. (2021)⁴ (4-OPA, 0.001-0.016; decanal, 0.012-0.02), Wisthaler and Weschler (2010) (4-OPA, 0.011; decanal, 0.051),² and Salvador et al.²⁰ (4-OPA, 0.038-0.092). Discrepancies between studies may be explained by the variability in yields between people,4 distribution in bathing frequency, 43 different experimental conditions (e.g., soiled clothing, clothing type, small skin reactor, field measurement) and analytical methods, and uncertainties in estimating absolute VOC mixing ratios.

The elevated per person O₃ deposition velocity indicates a higher ozone consumption rate. Along with moderately good agreements in molar yields with prior studies, it implies that the enhanced ozone consumption by occupants might cause elevated per person SOOP emission factors. The higher per person ozone consumption rate was potentially induced by the greater amount of SOOP precursors carried per person in the LL office than those in previous studies. We speculate that multiple layers of soiled clothing worn during the winter season in Indiana significantly increased the abundance of available precursors and surface area that can react with indoor O3, thereby leading to high ozone consumption rates and SOOP emission rates from the human envelope. Clothing likely contains skin oils and other condensed-phase SOOP precursors that can remove substantial amounts of O₃. 14,44 A previous study indicated that a single soiled T-shirt can result in a O₃ deposition velocity of 0.19-0.27 cm s⁻¹.⁴⁵ In addition, distributions in the laundry frequency for different textiles have shown that sweaters and jeans may be used for more than 10 days before being washed, while underpants and cotton Tshirts are likely washed after 1 or 2 days. 46,47 Therefore, it is possible that the laundry frequency can be relatively low (e.g., once or twice per season) for some winter clothing items, potentially making them heavily soiled and enriched with SOOP precursors. Although there is no literature directly demonstrating the influence of laundry frequency on SOOP emissions and ozone deposition, previous studies indicate that the ozone deposition velocity and ozone-initiated VOC emissions are higher for soiled clothing than for laundered clothing.48,49

Indoor Surface Emissions as a Significant Source of SOOPs in Office Environments. Indoor surface emissions were found to be a significant source of SOOPs in the LL office with a relatively stable net emission rate that was not depleted during the measurement campaign. Under the pre-existing HVAC operational mode, S_{surface} for 6-MHO, 4-OPA, and decanal were 294–1076, 155–1589, and 358–1408 μ g h⁻¹, respectively, with daily mean relative contributions to S_{total} of 0.13-0.38, 0.06-0.4, and 0.13-0.56, respectively. Tang et al. (2016)²³ reported nonoccupant indoor source rates of approximately 850 and 1400 $\mu g h^{-1}$ for 6-MHO and 4-OPA, respectively, in a university classroom. Another study in a university athletic center indicated that the interquartile ranges of the normalized surface emission rates (by total surface area) were 0.21–0.35, 2.1–2.9, and 0.25–0.44 μ g m⁻² h⁻¹ for 6-MHO, 4-OPA and decanal, respectively,²⁷ while the normalized net surface emission rates in the office were 0.42-3.10, 0.12-3.5, and $0.31-1.29 \mu g m^{-2} h^{-1}$, respectively. A recent study in a residential test house, which has a floor area similar to the office, exhibited relatively low emissions during unoccupied periods with mean emission rates of 105, 152, and 141 μ g h⁻¹ for 6-MHO, 4-OPA, and decanal, respectively.⁵⁰ Although volatile precursors (e.g., GA, 6-MHO) and condensed-phase skin oils can transfer to indoor surfaces via absorptive partitioning, 51,52 direct contact, and desquamation, 44 such high emission rates from indoor surfaces in the office are unlikely attributable to heterogeneous reactions between O₃ and condensed-phase precursors on indoor

We estimated the maximum production rates of SOOPs via heterogeneous reactions using O3 loss rates and the assumed maximum yields for indoor surfaces. For example, the O₃ loss rate to indoor surfaces during occupied periods was 6.7 μ mol h⁻¹ on February 27. Assuming a maximum yield of decanal for the indoor surface to be 0.024, which is the mean yield for office workers obtained in this study (Table S1), the estimated production rate of decanal via heterogeneous reactions is about 25 μ g h⁻¹, which only accounts for 4.4% of S_{surface} (592 μ g h⁻¹) on that day (Table S2). Considering the concentration of precursors on indoor surfaces to be much lower than that on human skin and clothing, the actual contribution might be negligible. In contrast, two recent studies indicated that offbody skin lipids on indoor surfaces contribute significantly to O₃ reactivity and SOOP emissions in a residential building and a university classroom with low indoor O_3 concentrations (mean of 4–6 ppb). Since the hard flooring in the LL office is cleaned frequently⁵⁴ and indoor O₃ concentrations were relatively high (typically 10-25 ppb), we do not expect a long persistence time scale for off-body skin lipids. Therefore, the ozonolysis of off-body skin lipids may not be an important SOOP source in routinely cleaned office environments with high outdoor air ventilation rates.

The consistent indoor surface emissions are likely due to the existence of a significant surface reservoir of SOOPs. In surface reservoirs, VOCs are stored in the condensed phase and can rapidly partition between the gas and the surface phases, thereby behaving as a persistent emission source. This is supported by several recent studies that observed continuous emissions from surface reservoirs by the repeatable "rebound" effect for a variety of gas molecules after "enhanced ventilation" experiments, absorptive partitioning of a wide range of organic molecules to indoor surfaces, and the growth of indoor organic films. Se-60 Wang et al. (2020) indicated that

many indoor gaseous contaminants mainly reside in surface reservoirs, rather than the gas phase. The primary surface reservoirs in the LL office may include the latex-painted walls (surface area = 365 m²),^{51,52} porous chair cushions, gypsum ceilings, organic films on each surface, and deposited particles. Aside from the hard tile floor, which is cleaned frequently, other surfaces were never routinely cleaned, potentially leading to thick layers of organic films and deposited particles that serve as a substantial surface reservoir for SOOPs.

The persistent surface emissions of SOOPs over the measurement period indicates that the gas molecules may diffuse deep into and strongly bond with the surface reservoirs. They then may slowly migrate to the gas—surface interface, creating a near-continuous flux to indoor air. Interestingly, to meet the criteria for LEED Gold certification, the office building and LL office were built with the goal of minimal to zero VOC emissions from building materials and furnishings. However, the large indoor surface reservoirs resulted in SOOP source rates comparable with occupant-associated SOOP source rates for this particular LEED office building. To improve indoor air quality in future high-performance and green buildings, advanced building technologies or engineering strategies are needed to minimize surface reservoirs and to reduce emissions from surface reservoirs. 61

The highest $S_{\rm surface}$ for all three SOOPs was observed on March 14, when the RR transitioned from 1 (from March 6 to March 13) to 0 during implementation of the override HVAC mode (Figure S2). $S_{\rm surface}$ decreased significantly from 2179–2511 μ g h⁻¹ on March 14 to 1076–1589 μ g h⁻¹ on March 15 but remained much higher than on days prior to March 13. $S_{\rm surface}$ was the lowest on March 12 for 4-OPA and decanal, when RR = 1. We hypothesize that the observed transitions in $S_{\rm surface}$ can be attributed to enhanced sorption of gas-phase SOOPs when indoor concentrations are elevated under RR = 1 (Table S2), followed by rapid desorption as RR drops to 0.

The partitioning between the gas phase and surface reservoir is typically treated as a sorption and desorption process. 62-64 In this study, we simplified the two processes with a net surface emission rate as we did not observe an obvious sorption effect during the decay in SOOP concentrations during unoccupied periods (Figure S3). This was not even observed when RR = 1(Figure S3a-c), potentially because the sorption rate was low compared to the AER of 7.1 h⁻¹. The net emission rate from the surface reservoir should be driven by a deviation from equilibrium between the surface concentration of the reservoir and the gas-phase concentration. We observed moderate negative correlations between the net surface emission rate and the indoor SOOP concentrations (Figure S4), suggesting that the driving force from the surface reservoir to the gas phase was small at high indoor concentrations, resulting in low net surface emission rates. The elevated indoor SOOP concentrations due to RR = 1 from March 6 to March 13 may enhance the sorption effect of gas-phase SOOPs and lead to an increased concentration in the surface reservoir during this period.

The LL office temperature increased 2-6 °C when RR = 1 due to the lack of cool outdoor air. The increased temperature can enhance VOC emissions from building materials and furnishings. However, this is not reflected by the net surface emission rate, further indicating the potential sorption effect when RR = 1. When the RR shifted to 0 on March 14, indoor SOOP concentrations decreased dramatically due to the dilution of outdoor air, which weakened the sorption effect

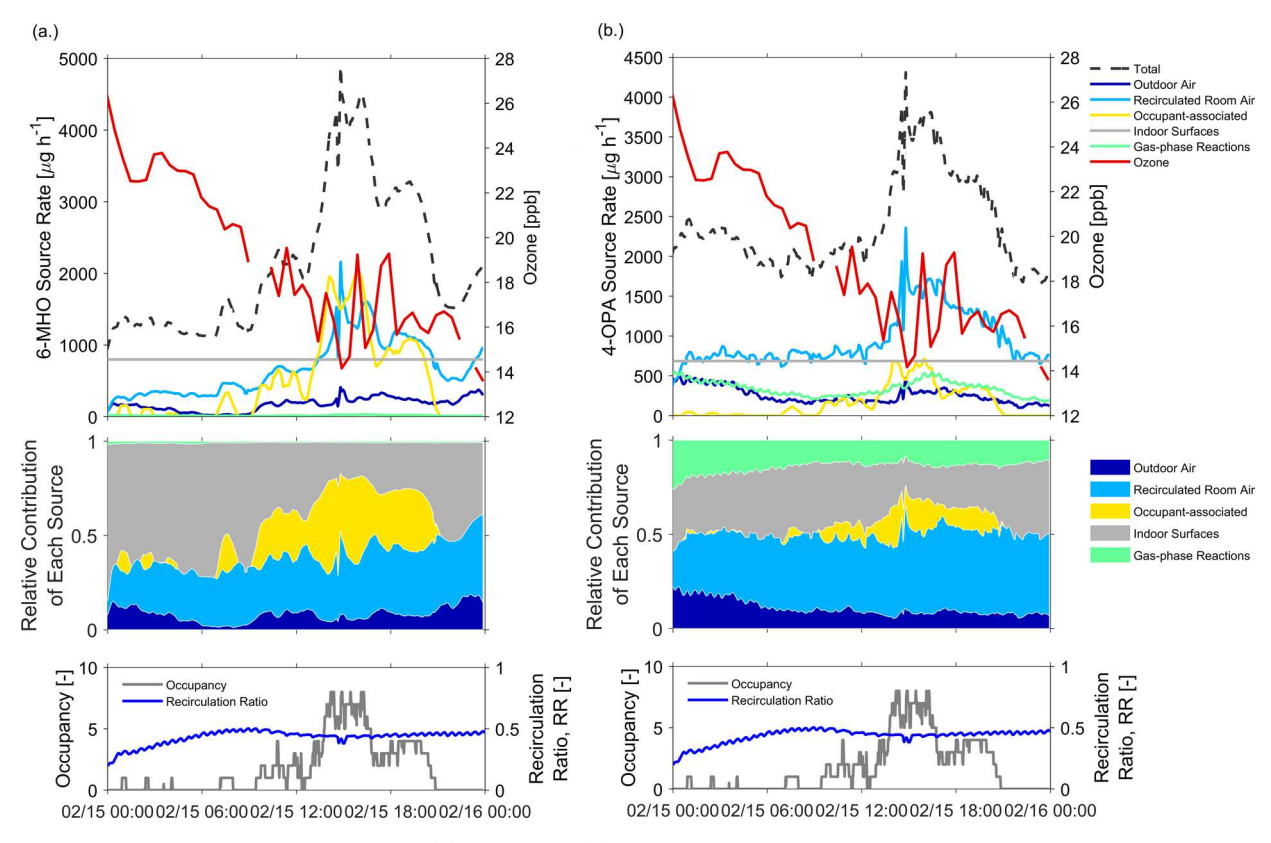


Figure 2. Diurnal variations in the source rates for (a) 6-MHO and (b) 4-OPA on February 15, 2019. The top plots show the time-resolved source-specific SOOP source rates, total SOOP source rates, and the indoor O_3 concentration time series. The middle plots show the relative contribution of each source type to the total SOOP source rate. The bottom plots show the office occupancy and recirculation ratio time series.

and increased the deviation from equilibrium between the increased concentration in the surface reservoir and indoor air. This resulted in a significantly enhanced net emission on March 14. Since the RR was only maintained at 1 for 1 week, the deposited molecules may not diffuse deep into the surface reservoir and instead stay relatively close to the surface. Following the first day of enhanced emissions (March 15), the abundance of molecules near the surface of the reservoir is possibly reduced, resulting in the lower net surface emission rate observed on March 15. It is also possible that SVOC concentrations increased when RR = 1, which facilitated the growth of organic films and increased the absorptive capacity of the film to allow more SOOPs to absorb, later resulting in the elevated net surface emission rate. ^{58–60}

Dynamic Features of SOOP Source Rates in the Living Laboratory Office. Real-time monitoring of office occupancy and HVAC system operational conditions coupled with multilocation VOC sampling via PTR-TOF-MS enables investigation of the dynamic features of SOOP source rates in the LL office. Figure 2 presents the temporal evolution of source rates for 6-MHO and 4-OPA on February 15, along with occupancy, RR, and indoor O₃ concentrations. The sinusoidal-like variation in RR indicates that the dampers are constantly adjusting through the building automation feedback control to maintain the mixed air temperature set point. Due to the decrease in outdoor air temperature (Figure S2), the RR changed from about 0.2 at 12 AM to about 0.48 at 8 AM. This induced a drop in both $S_{\rm outdoor}$ and the indoor O_3 concentration. The latter contributed to a decrease in $S_{\text{gas-rxn}}$ for 4-OPA from 518 to 218 μ g h⁻¹.

 S_{human} exhibited high temporal variations associated with office occupancy (Figure 2). S_{human} reached a maximum of 1950 and 683 μ g h⁻¹ for 6-MHO and 4-OPA, respectively, when 8 office workers were present in the LL office. S_{recirc} and S_{eas-rxn} also increased with occupancy due to emissions from the human envelope, leading to increased concentrations of gas-phase precursors. The rise in S_{recirc} showed a relatively short time delay after the increase in occupancy, while that of S_{gas-rxn} for 4-OPA presented a longer time delay as it is a secondary SOOP. The impact of occupancy and ventilation mode on the relative contribution of each SOOP source type is presented in the middle plots of Figure 2. When the office occupancy was high, S_{recirc} and S_{human} dominated S_{total} for 6-MHO, while S_{surface} dominated during unoccupied periods. For 4-OPA, indoor surface emissions and recirculation air were the two dominant sources, while S_{human} only contributed up to 0.21 when occupancy was high. $S_{\rm total}$ values during unoccupied periods were 1350–2000 and 1700–2400 $\mu \rm g~h^{-1}$ for 6-MHO and 4-OPA, respectively, while S_{total} reached 4800 and 4300 μ g h⁻¹ for the highest occupancy periods, respectively.

Influence of the HVAC System Recirculation Ratio and Office Occupancy on Indoor SOOP Concentrations. Figure 3a and 3b present the concentration of decanal and 6-MHO as a function of office occupancy. The size and color of the circular markers indicate the RR and indoor O₃ concentration, respectively, for data collected prior to March 13. The size and color of the triangular markers indicate the RR and indoor O₃ concentration, respectively, for data collected on March 14 and 15 when an enhanced S_{surface} was observed. The concentrations of 6-MHO and decanal generally increased with occupancy in the LL office. At a given

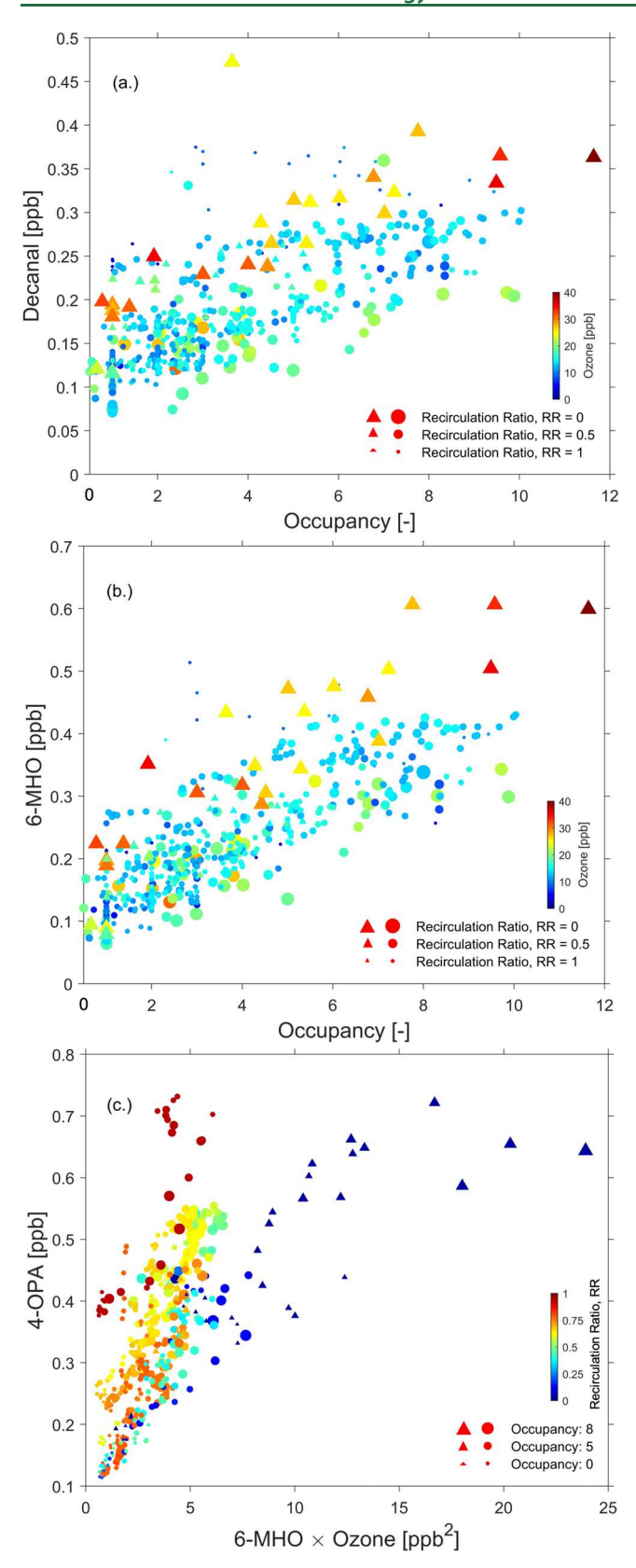


Figure 3. Indoor concentrations of (a) decanal and (b) 6-MHO as a function of office occupancy. Size and color of the circular markers indicate the recirculation ratio and indoor O3 concentration, respectively, for data collected prior to March 13, 2019. Size and color of the triangular markers indicate the recirculation ratio and indoor O₃ concentration, respectively, for data collected on March 14 and 15, 2019 when enhanced S_{surface} was observed. (c) Indoor

Figure 3. continued

concentrations of 4-OPA as a function of the product of 6-MHO concentrations and indoor O3 concentrations. Size and color of the circular markers indicate the occupancy and recirculation ratio, respectively, for data collected prior to March 13, 2019. Size and color of the triangular markers indicate the occupancy and recirculation ratio, respectively, for data collected on March 14 and 15, 2019 when enhanced S_{surface} was observed.

occupancy, concentrations varied by about 0.15-0.2 ppb, with the small blue circular markers appearing in the upper regions and the large green circular markers appearing in the lower regions. This indicates that the 6-MHO and decanal concentrations increased with the RR and that the increase in S_{recirc} outcompeted the decrease in S_{human} induced by the lower indoor O₃ concentrations. High concentrations of 6-MHO and decanal were also observed when RR = 0 for measurements on March 14 and 15 (triangular markers). Concentrations were similar to those measured before March 13 when RR = 1. This is due to the enhanced S_{surface} observed on March 14 and 15 (for reasons previously discussed) and an increase in S_{human} due to high indoor O₃ concentrations under 100% outdoor air.

Figure 3c presents the correlation between the concentration of 4-OPA and the product of its precursor, 6-MHO, and indoor O3 concentrations. Here, the size and color of the circular markers indicate the occupancy and RR, respectively, for data collected prior to March 13. The size and color of the triangular markers indicate the occupancy and RR, respectively, for data collected on March 14 and 15. With RR shifting from 0 to 1 (blue to red), the scattered circular markers move upward due to the increased amount of recirculated SOOPs. Similar to 6-MHO and decanal, the highest concentrations of 4-OPA were observed for RR = 1 for measurements before March 13 (red circular markers) and for RR = 0 for measurements on March 14 and 15 (blue triangular markers). The latter is due to the increase in S_{surface} observed on March 14 and 15. Collectively, the SOOP concentrations and source rates for the LL office demonstrate the important role of building factors along with occupancy and gas- and surfacebased processes in influencing indoor air chemistry in offices. To reduce total source rates of SOOPs and occupant exposure to SOOPs, carbon-based filters and catalytic devices can be installed in the HVAC system to minimize ozone concentrations in the supply air $^{70-75}$ trations in the supply air.

Study Limitations. A limitation of this study is that the partitioning of SOOPs between indoor surfaces and the gas phase was evaluated in a simplified manner through the use of a net surface emission rate. However, day-to-day variations in the net surface emission rate suggest that dynamic sorption and desorption processes are influenced by SOOP concentrations in the gas and surface phases. As the gas-phase concentrations exhibited strong temporal variation through the day, the net mass flux of the SOOPs from the surface reservoir to indoor air potentially varied accordingly and transiently. For example, elevated concentrations in the office during highoccupancy periods might reduce the driving force of the surface-to-air mass flux. Therefore, the source rate for surfacerelated emissions is variable in reality. In addition, enhanced surface emissions on March 14 and 15 suggest temporal changes in the thickness, SOOP concentration profile, and SOOP diffusion within the surface reservoirs. These processes

have been observed during temporally resolved direct measurements of gas- and surface-phase VOCs. ^{25,51,52} However, such processes were not incorporated into the current model as key parameters were unknown, such as the SOOP diffusion coefficient and the effective thickness of the reservoir. In addition, how indoor surfaces evolve over long time scales from a sink for VOCs (e.g., for a newly built building) ^{51,62} into a large emission reservoir (e.g., for an occupied building) remains unknown. ⁵² Although many experiments have characterized sorption and desorption processes of VOCs onto various indoor materials for relatively short time scales, ^{51,64,76–78} long-term characterization of the interaction between gas- and surface-phase VOCs is needed.

Long PFA sample lines (\sim 20 m) were used in this study. PFA tubing performs better than other polymeric tubing in preventing absorptive partitioning of VOCs, and the sample lines were continuously purged during the multilocation sampling. However, there may be some amount of sorption of VOCs to the PFA sample lines⁷⁹ which cannot be corrected in this study. The long sample lines may also allow for reactions between O₃ and gas-phase or surface-absorbed GA and 6-MHO. However, since the residence time in the sample lines was <4 s, we did not expect such reactions to meaningfully influence the estimated concentrations. The mixing conditions of room air may have some effect on the fitted results. Since emissions from the human envelope can be viewed as a "point" source, 80 if the room air is not well mixed, the proposed material balance model may not represent realistic conditions. The rapid changes in occupancy may result in uneven distributions in local SOOP concentrations. If the mixing intensity is too weak, the changes in concentration may not be detected by the instrument immediately, since the room air was sampled from the return air duct. This will affect the fitting quality of the model. However, as the overall air exchange rate was high during the campaign, we do not expect the mixing intensity to be too weak. Therefore, it may not significantly affect the modeled results.

In this study, the emission rates from heterogeneous reactions on the human surface envelope were expressed as $k_{\text{app,i}}[O_3]$, which is based on the assumption that the concentration and abundance of condensed-phase precursors from an occupant are constant. Such a manner simplified the model and helped us focus on the impact of occupancy and mechanical ventilation on SOOP source rates. However, it is realized that the concentrations of precursors in the condensed phase may change with time and vary between individuals. The available skin oil for heterogeneous reactions is potentially affected by many factors, such as the exposed area of human skin, 14 indoor ozone concentration (affecting the abundance of accumulated precursors), production rate of the skin oil, degree of soiling of the garment, 49 and use of personal care products. In addition, 4-OPA and 6-MHO can be produced as second-generation products from the human surface envelope via ozonolysis of the condensed-phase first-generation SOOPs, which could be both low-volatility (e.g., C27-pentaenal and C22-tetraenal) and high-volatility (e.g., GA and OH-6-MHO) compounds.² Their concentrations can be affected by a series of complex chemical and physical processes. To focus on understanding these processes, more complicated models can be adopted. 14,15

ASSOCIATED CONTENT

Supporting Information

The Supporting Information is available free of charge at https://pubs.acs.org/doi/10.1021/acs.est.1c03112.

Detailed description of the Herrick Living Laboratory offices and their HVAC systems, calibration and operation of the PTR-TOF-MS, automated valve system for multilocation sampling across the Living Laboratory HVAC system, and supplemental results for the indoor SOOP concentrations and source rates (PDF)

AUTHOR INFORMATION

Corresponding Author

Brandon E. Boor — Lyles School of Civil Engineering, Purdue University, West Lafayette, Indiana 47907, United States; Ray W. Herrick Laboratories, Center for High Performance Buildings, Purdue University, West Lafayette, Indiana 47907, United States; orcid.org/0000-0003-1011-4100; Email: bboor@purdue.edu

Authors

Tianren Wu — Lyles School of Civil Engineering, Purdue University, West Lafayette, Indiana 47907, United States; Ray W. Herrick Laboratories, Center for High Performance Buildings, Purdue University, West Lafayette, Indiana 47907, United States; orcid.org/0000-0001-9214-3719

Antonios Tasoglou — RJ Lee Group Incorporated, Monroeville, Pennsylvania 15146, United States; orcid.org/0000-0001-9767-5343

Heinz Huber — Edelweiss Technology Solutions, Limited Liability Company, Novelty, Ohio 44072, United States Philip S. Stevens — O'Neill School of Public and Environmental Affairs, Indiana University, Bloomington, Indiana 47405, United States; Department of Chemistry, Indiana University, Bloomington, Indiana 47405, United States; orcid.org/0000-0001-9899-4215

Complete contact information is available at: https://pubs.acs.org/10.1021/acs.est.1c03112

Notes

The authors declare no competing financial interest.

ACKNOWLEDGMENTS

Financial support was provided by the National Science Foundation (CBET-1805804) and the Alfred P. Sloan Foundation Chemistry of Indoor Environments Program (G-2018-11061).

REFERENCES

- (1) Weschler, C. J. Ozone in Indoor Environments: Concentration and Chemistry. *Indoor Air* **2000**, *10* (4), 269–288.
- (2) Wisthaler, A.; Weschler, C. J. Reactions of Ozone with Human Skin Lipids: Sources of Carbonyls, Dicarbonyls, and Hydroxycarbonyls in Indoor Air. *Proc. Natl. Acad. Sci. U. S. A.* **2010**, *107* (15), 6568–6575
- (3) Zhou, S.; Forbes, M. W.; Abbatt, J. P. D. Kinetics and Products from Heterogeneous Oxidation of Squalene with Ozone. *Environ. Sci. Technol.* **2016**, *50* (21), 11688–11697.
- (4) Morrison, G. C.; Eftekhari, A.; Majluf, F.; Krechmer, J. E. Yields and Variability of Ozone Reaction Products from Human Skin. *Environ. Sci. Technol.* **2021**, *55* (1), 179–187.

- (5) Guadagni, D. G.; Buttery, R. G.; Okano, S. Odour Thresholds of Some Organic Compounds Associated with Food Flavours. *J. Sci. Food Agric.* **1963**, *14* (10), 761–765.
- (6) Jarvis, J.; Seed, M. J.; Elton, R.; Sawyer, L.; Agius, R. Relationship between Chemical Structure and the Occupational Asthma Hazard of Low Molecular Weight Organic Compounds. *Occup. Environ. Med.* **2005**, *62* (4), 243–250.
- (7) Anderson, S. E.; Franko, J.; Jackson, L. G.; Wells, J. R.; Ham, J. E.; Meade, B. J. Irritancy and Allergic Responses Induced by Exposure to the Indoor Air Chemical 4-Oxopentanal. *Toxicol. Sci.* **2012**, *127* (2), 371–381.
- (8) Anderson, S. E.; Wells, J. R.; Fedorowicz, A.; Butterworth, L. F.; Meade, B. J.; Munson, A. E. Evaluation of the Contact and Respiratory Sensitization Potential of Volatile Organic Compounds Generated by Simulated Indoor Air Chemistry. *Toxicol. Sci.* **2007**, 97 (2), 355–363.
- (9) Anderson, S. E.; Jackson, L. G.; Franko, J.; Wells, J. R. Evaluation of Dicarbonyls Generated in a Simulated Indoor Air Environment Using an in Vitro Exposure System. *Toxicol. Sci.* **2010**, *115* (2), 453–461
- (10) Avery, A. M.; Waring, M. S.; DeCarlo, P. F. Human Occupant Contribution to Secondary Aerosol Mass in the Indoor Environment. *Environ. Sci. Process. Impacts* **2019**, 21 (8), 1301–1312.
- (11) Ottaviani, M.; Alestas, T.; Flori, E.; Mastrofrancesco, A.; Zouboulis, C. C.; Picardo, M. Peroxidated Squalene Induces the Production of Inflammatory Mediators in HaCaT Keratinocytes: A Possible Role in Acne Vulgaris. *J. Invest. Dermatol.* **2006**, *126* (11), 2430–2437.
- (12) Chiba, K.; Yoshizawa, K.; Makino, I.; Kawakami, K.; Onoue, M. Comedogenicity of Squalene Monohydroperoxide in the Skin after Topical Application. *J. Toxicol. Sci.* **2000**, *25* (2), 77–83.
- (13) Saint-Leger, D.; Bague, A.; Lefebvre, E.; Cohen, E.; Chivot, M. A Possible Role for Squalene in the Pathogenesis of Acne. II. In Vivo Study of Squalene Oxides in Skin Surface and Intra-comedonal Lipids of Acne Patients. *Br. J. Dermatol.* **1986**, *114* (5), 543–552.
- (14) Lakey, P. S. J.; Morrison, G. C.; Won, Y.; Parry, K. M.; von Domaros, M.; Tobias, D. J.; Rim, D.; Shiraiwa, M. The Impact of Clothing on Ozone and Squalene Ozonolysis Products in Indoor Environments. *Commun. Chem.* **2019**, 2 (1), 56.
- (15) Lakey, P. S. J.; Wisthaler, A.; Berkemeier, T.; Mikoviny, T.; Pöschl, U.; Shiraiwa, M. Chemical Kinetics of Multiphase Reactions between Ozone and Human Skin Lipids: Implications for Indoor Air Quality and Health Effects. *Indoor Air* 2017, 27 (4), 816–828.
- (16) Agarwal, Y.; Balaji, B.; Gupta, R.; Lyles, J.; Wei, M.; Weng, T. Occupancy-Driven Energy Management for Smart Building Automation. In Proceedings of the 2nd ACM Workshop on Embedded Sensing Systems for Energy-Efficiency in Buildings, 2010; pp 1–6.
- (17) Erickson, V. L.; Cerpa, A. E. Occupancy Based Demand Response HVAC Control Strategy. In Proceedings of the 2nd ACM Workshop on Embedded Sensing Systems for Energy-Efficiency in Buildings 2010, 7–12.
- (18) Afram, A.; Janabi-Sharifi, F. Theory and Applications of HVAC Control Systems-A Review of Model Predictive Control (MPC). *Build. Environ.* **2014**, *72*, 343–355.
- (19) Weschler, C. J.; Wisthaler, A.; Cowlin, S.; Tamás, G.; Strøm-Tejsen, P.; Hodgson, A. T.; Destaillats, H.; Herrington, J.; Zhang, J.; Nazaroff, W. W. Ozone-Initiated Chemistry in an Occupied Simulated Aircraft Cabin. *Environ. Sci. Technol.* **2007**, 41 (17), 6177–6184.
- (20) Salvador, C. M.; Bekö, G.; Weschler, C. J.; Morrison, G.; Le Breton, M.; Hallquist, M.; Ekberg, L.; Langer, S. Indoor Ozone/Human Chemistry and Ventilation Strategies. *Indoor Air* **2019**, 29 (6), 913–925.
- (21) Wisthaler, A.; Tamás, G.; Wyon, D. P.; Strøm-Tejsen, P.; Space, D.; Beauchamp, J.; Hansel, A.; Märk, T. D.; Weschler, C. J. Products of Ozone-Initiated Chemistry in a Simulated Aircraft Environment. *Environ. Sci. Technol.* **2005**, 39 (13), 4823–4832.
- (22) Bekö, G.; Wargocki, P.; Wang, N.; Li, M.; Weschler, C. J.; Morrison, G.; Langer, S.; Ernle, L.; Licina, D.; Yang, S. The Indoor Chemical Human Emissions and Reactivity (ICHEAR) Project:

- Overview of Experimental Methodology and Preliminary Results. *Indoor Air* **2020**, *30*, 1213–1228.
- (23) Tang, X.; Misztal, P. K.; Nazaroff, W. W.; Goldstein, A. H. Volatile Organic Compound Emissions from Humans Indoors. *Environ. Sci. Technol.* **2016**, *50* (23), 12686–12694.
- (24) Liu, S.; Li, R.; Wild, R. J.; Warneke, C.; de Gouw, J. A.; Brown, S. S.; Miller, S. L.; Luongo, J. C.; Jimenez, J. L.; Ziemann, P. J. Contribution of Human-related Sources to Indoor Volatile Organic Compounds in a University Classroom. *Indoor Air* **2016**, *26* (6), 925–938.
- (25) Pagonis, D.; Price, D.; Algrim, L. B.; Day, D. A.; Handschy, A.; Stark, H.; Miller, S. L.; de Gouw, J. A.; Jimenez, J. L.; Ziemann, P. J. Time-Resolved Measurements of Indoor Chemical Emissions, Deposition, and Reactions in a University Art Museum. *Environ. Sci. Technol.* **2019**, 53 (9), 4794–4802.
- (26) Stönner, C.; Edtbauer, A.; Williams, J. Real-world Volatile Organic Compound Emission Rates from Seated Adults and Children for Use in Indoor Air Studies. *Indoor Air* 2018, 28 (1), 164–172.
- (27) Finewax, Z.; Pagonis, D.; Claflin, M. S.; Handschy, A. V.; Brown, W. L.; Jenks, O.; Nault, B. A.; Day, D. A.; Lerner, B. M.; Jimenez, J. L.; et al. Quantification and Source Characterization of Volatile Organic Compounds from Exercising and Application of Chlorine-based Cleaning Products in a University Athletic Center. *Indoor Air* 2021, 31, 1323–1339.
- (28) Liu, Y.; Misztal, P. K.; Xiong, J.; Tian, Y.; Arata, C.; Weber, R. J.; Nazaroff, W. W.; Goldstein, A. H. Characterizing Sources and Emissions of Volatile Organic Compounds in a Northern California Residence Using Space-and Time-resolved Measurements. *Indoor Air* **2019**, 29 (4), 630–644.
- (29) Liu, Y.; Misztal, P. K.; Arata, C.; Weschler, C. J.; Nazaroff, W. W.; Goldstein, A. H. Observing Ozone Chemistry in an Occupied Residence. *Proc. Natl. Acad. Sci. U. S. A.* **2021**, *118* (6), No. e2018140118.
- (30) Wagner, D. N.; Mathur, A.; Boor, B. E. Spatial Seated Occupancy Detection in Offices with a Chair-Based Temperature Sensor Array. *Build. Environ.* **2021**, *187*, 107360.
- (31) Xiong, J.; He, Z.; Tang, X.; Misztal, P. K.; Goldstein, A. H. Modeling the Time-Dependent Concentrations of Primary and Secondary Reaction Products of Ozone with Squalene in a University Classroom. *Environ. Sci. Technol.* **2019**, 53 (14), 8262–8270.
- (32) US EPA. Estimation Programs Interface SuiteTM for Microsoft® Windows, v 4.11; United States EPA: Washington, DC, USA, 2012.
- (33) Weschler, C. J.; Shields, H. C. Measurements of the Hydroxyl Radical in a Manipulated but Realistic Indoor Environment. *Environ. Sci. Technol.* **1997**, 31 (12), 3719–3722.
- (34) Sarwar, G.; Corsi, R.; Kimura, Y.; Allen, D.; Weschler, C. J. Hydroxyl Radicals in Indoor Environments. *Atmos. Environ.* **2002**, *36* (24), 3973–3988.
- (35) Gomez Alvarez, E.; Amedro, D.; Afif, C.; Gligorovski, S.; Schoemaecker, C.; Fittschen, C.; Doussin, J.-F.; Wortham, H. Unexpectedly High Indoor Hydroxyl Radical Concentrations Associated with Nitrous Acid. *Proc. Natl. Acad. Sci. U. S. A.* **2013**, *110*, 13294–13299.
- (36) Carslaw, N. A New Detailed Chemical Model for Indoor Air Pollution. *Atmos. Environ.* **2007**, *41* (6), 1164–1179.
- (37) Du Bois, D. A Formula to Estimate the Approximate Surface Area If Height and Weight Be Known. *Nutrition* 1989, 5, 303–313.
- (38) Lai, D.; Karava, P.; Chen, Q. Study of Outdoor Ozone Penetration into Buildings through Ventilation and Infiltration. *Build. Environ.* **2015**, 93, 112–118.
- (39) Nazaroff, W. W.; Gadgil, A. J.; Weschler, C. J. Critique of the Use of Deposition Velocity in Modeling Indoor Air Quality. *Modeling of Indoor Air Quality and Exposure*; ASTM International, 1993; pp 81–104.
- (40) Fadeyi, M. O.; Weschler, C. J.; Tham, K. W.; Wu, W. Y.; Sultan, Z. M. Impact of Human Presence on Secondary Organic Aerosols Derived from Ozone-Initiated Chemistry in a Simulated Office Environment. *Environ. Sci. Technol.* **2013**, 47 (8), 3933–3941.

- (41) Tamas, G.; Weschler, C. J.; Bako-Biro, Z.; Wyon, D. P.; Strøm-Tejsen, P. Factors Affecting Ozone Removal Rates in a Simulated Aircraft Cabin Environment. *Atmos. Environ.* **2006**, 40 (32), 6122–6133.
- (42) Yang, S.; Gao, K.; Yang, X. Volatile Organic Compounds (VOCs) Formation Due to Interactions between Ozone and Skin-Oiled Clothing: Measurements by Extraction-Analysis-Reaction Method. *Build. Environ.* **2016**, *103*, 146–154.
- (43) Wilkes, C. R.; Mason, A. D.; Hern, S. C. Probability Distributions for Showering and Bathing Water-use Behavior for Various US Subpopulations. *Risk Anal. An Int. J.* **2005**, 25 (2), 317–337.
- (44) Weschler, C. J. Roles of the Human Occupant in Indoor Chemistry. *Indoor Air* **2016**, 26 (1), 6–24.
- (45) Fischer, A.; Ljungström, E.; Langer, S. Ozone Removal by Occupants in a Classroom. *Atmos. Environ.* **2013**, *81*, 11–17.
- (46) Laitala, K.; Klepp, I. G.; Boks, C. Changing Laundry Habits in Norway. *Int. J. Consum. Stud.* **2012**, 36 (2), 228–237.
- (47) Jack, T. Nobody Was Dirty: Intervening in Inconspicuous Consumption of Laundry Routines. *J. Consum. Cult.* **2013**, *13* (3), 406–421.
- (48) Coleman, B. K.; Destaillats, H.; Hodgson, A. T.; Nazaroff, W. W. Ozone Consumption and Volatile Byproduct Formation from Surface Reactions with Aircraft Cabin Materials and Clothing Fabrics. *Atmos. Environ.* **2008**, *42* (4), 642–654.
- (49) Rai, A. C.; Guo, B.; Lin, C.; Zhang, J.; Pei, J.; Chen, Q. Ozone Reaction with Clothing and Its Initiated VOC Emissions in an Environmental Chamber. *Indoor Air* **2014**, 24 (1), 49–58.
- (50) Arata, C.; Misztal, P. K.; Tian, Y.; Lunderberg, D. M.; Kristensen, K.; Novoselac, A.; Vance, M. E.; Farmer, D. K.; Nazaroff, W. W.; Goldstein, A. H. Volatile Organic Compound Emissions during HOMEChem. *Indoor Air* **2021**, *31*, 2099–2117.
- (51) Algrim, L. B.; Pagonis, D.; de Gouw, J. A.; Jimenez, J. L.; Ziemann, P. J. Measurements and Modeling of Absorptive Partitioning of Volatile Organic Compounds to Painted Surfaces. *Indoor Air* **2020**, *30* (4), 745–756.
- (52) Wang, C.; Collins, D. B.; Arata, C.; Goldstein, A. H.; Mattila, J. M.; Farmer, D. K.; Ampollini, L.; DeCarlo, P. F.; Novoselac, A.; Vance, M. E.; et al. Surface Reservoirs Dominate Dynamic Gas-Surface Partitioning of Many Indoor Air Constituents. *Sci. Adv.* 2020, 6 (8), No. eaay8973.
- (53) Zhang, M.; Xiong, J.; Liu, Y.; Misztal, P. K.; Goldstein, A. H. Physical-Chemical Coupling Model for Characterizing the Reaction of Ozone with Squalene in Realistic Indoor Environments. *Environ. Sci. Technol.* **2021**, *55* (3), 1690–1698.
- (54) Patra, S. S.; Wu, T.; Wagner, D. N.; Jiang, J.; Boor, B. E. Real-Time Measurements of Fluorescent Aerosol Particles in a Living Laboratory Office Under Variable Human Occupancy and Ventilation Conditions. *Build. Environ.* **2021**, 205, 108249.
- (55) Weschler, C. J.; Nazaroff, W. W. Semivolatile Organic Compounds in Indoor Environments. *Atmos. Environ.* **2008**, 42 (40), 9018–9040.
- (56) Singer, B. C.; Revzan, K. L.; Hotchi, T.; Hodgson, A. T.; Brown, N. J. Sorption of Organic Gases in a Furnished Room. *Atmos. Environ.* **2004**, *38* (16), 2483–2494.
- (57) Singer, B. C.; Hodgson, A. T.; Hotchi, T.; Ming, K. Y.; Sextro, R. G.; Wood, E. E.; Brown, N. J. Sorption of Organic Gases in Residential Rooms. *Atmos. Environ.* **2007**, *41* (15), 3251–3265.
- (58) Eichler, C. M. A.; Cao, J.; Isaacman-VanWertz, G.; Little, J. C. Modeling the Formation and Growth of Organic Films on Indoor Surfaces. *Indoor Air* **2019**, *29* (1), 17–29.
- (59) Weschler, C. J.; Nazaroff, W. W. Growth of Organic Films on Indoor Surfaces. *Indoor Air* **2017**, 27 (6), 1101–1112.
- (60) Lim, C. Y.; Abbatt, J. P. Chemical Composition, Spatial Homogeneity, and Growth of Indoor Surface Films. *Environ. Sci. Technol.* **2020**, *54* (22), 14372–14379.
- (61) Thevenet, F.; Debono, O.; Rizk, M.; Caron, F.; Verriele, M.; Locoge, N. VOC Uptakes on Gypsum Boards: Sorption Performances

- and Impact on Indoor Air Quality. Build. Environ. 2018, 137, 138–146.
- (62) Tichenor, B. A.; Guo, Z.; Dunn, J. E.; Sparks, L. E.; Mason, M. A. The Interaction of Vapour Phase Organic Compounds with Indoor Sinks. *Indoor Air* **1991**, *1* (1), 23–35.
- (63) Van Loy, M. D.; Riley, W. J.; Daisey, J. M.; Nazaroff, W. W. Dynamic Behavior of Semivolatile Organic Compounds in Indoor Air. 2. Nicotine and Phenanthrene with Carpet and Wallboard. *Environ. Sci. Technol.* **2001**, *35* (3), 560–567.
- (64) Won, D.; Sander, D. M.; Shaw, C. Y.; Corsi, R. L. Validation of the Surface Sink Model for Sorptive Interactions between VOCs and Indoor Materials. *Atmos. Environ.* **2001**, *35* (26), 4479–4488.
- (65) Boor, B. E.; Järnström, H.; Novoselac, A.; Xu, Y. Infant Exposure to Emissions of Volatile Organic Compounds from Crib Mattresses. *Environ. Sci. Technol.* **2014**, *48* (6), 3541–3549.
- (66) Van der Wal, J. F.; Hoogeveen, A. W.; Wouda, P. The Influence of Temperature on the Emission of Volatile Organic Compounds from PVC Flooring, Carpet, and Paint. *Indoor Air* **1997**, 7 (3), 215–221.
- (67) Masuck, I.; Hutzler, C.; Jann, O.; Luch, A. Inhalation Exposure of Children to Fragrances Present in Scented Toys. *Indoor Air* **2011**, 21 (6), 501–511.
- (68) Lin, C.-C.; Yu, K.-P.; Zhao, P.; Whei-May Lee, G. Evaluation of Impact Factors on VOC Emissions and Concentrations from Wooden Flooring Based on Chamber Tests. *Build. Environ.* **2009**, *44* (3), 525–533.
- (69) Haghighat, F.; De Bellis, L. Material Emission Rates: Literature Review, and the Impact of Indoor Air Temperature and Relative Humidity. *Build. Environ.* **1998**, 33 (5), 261–277.
- (70) Yang, S.; Zhu, Z.; Wei, F.; Yang, X. Carbon Nanotubes/ Activated Carbon Fiber Based Air Filter Media for Simultaneous Removal of Particulate Matter and Ozone. *Build. Environ.* **2017**, *125*, 60–66.
- (71) Cros, C. J.; Morrison, G. C.; Siegel, J. A.; Corsi, R. L. Long-Term Performance of Passive Materials for Removal of Ozone from Indoor Air. *Indoor Air* **2012**, 22 (1), 43–53.
- (72) Metts, T. A.; Batterman, S. A. Effect of VOC Loading on the Ozone Removal Efficiency of Activated Carbon Filters. *Chemosphere* **2006**, 62 (1), 34–44.
- (73) Aldred, J. R.; Darling, E.; Morrison, G.; Siegel, J.; Corsi, R. L. Benefit-Cost Analysis of Commercially Available Activated Carbon Filters for Indoor Ozone Removal in Single-Family Homes. *Indoor Air* **2016**, *26* (3), 501–512.
- (74) Lee, P.; Davidson, J. Evaluation of Activated Carbon Filters for Removal of Ozone at the PPB Level. *Am. Ind. Hyg. Assoc. J.* **1999**, *60* (5), 589–600.
- (75) Wu, F.; Lu, Y.; Wang, M.; Zhang, X.; Yang, C. Catalytic Removal of Ozone by Pd/ACFs and Optimal Design of Ozone Converter for Air Purification in Aircraft Cabin. *Civ. Eng. J.* **2019**, 5 (8), 1656–1671.
- (76) Colombo, A.; De Bortoli, M.; Knoppel, H.; Pecchio, E.; Vissers, H. Adsorption of Selected Volatile Organic Compounds on a Carpet, a Wall Coating, and a Gypsum Board in a Test Chamber. *Indoor Air* **1993**, 3 (4), 276–282.
- (77) Jørgensen, R. B.; Bjørseth, O.; Malvik, B. Chamber Testing of Adsorption of Volatile Organic Compounds (VOCs) on Material Surfaces. *Indoor Air* **1999**, 9 (1), 2–9.
- (78) Ongwandee, M.; Morrison, G. C. Influence of Ammonia and Carbon Dioxide on the Sorption of a Basic Organic Pollutant to Carpet and Latex-Painted Gypsum Board. *Environ. Sci. Technol.* **2008**, 42 (15), 5415–5420.
- (79) Deming, B. L.; Pagonis, D.; Liu, X.; Day, D. A.; Talukdar, R.; Krechmer, J. E.; de Gouw, J. A.; Jimenez, J. L.; Ziemann, P. J. Measurements of Delays of Gas-Phase Compounds in a Wide Variety of Tubing Materials Due to Gas-Wall Interactions. *Atmos. Meas. Tech.* **2019**, *12* (6), 3453–3461.
- (80) Won, Y.; Lakey, P. S. J.; Morrison, G.; Shiraiwa, M.; Rim, D. Spatial Distributions of Ozonolysis Products from Human Surfaces in Ventilated Rooms. *Indoor Air* **2020**, *30* (6), 1229–1240.